Applied Catalysis B: Environmental 100 (2010) 221–228

Contents lists available at ScienceDirect

Applied Catalysis B: Environmental

journal homepage: www.elsevier.com/locate/apcatb

# Degradation of metronidazole by nanoscale zero-valent metal prepared from steel pickling waste liquor

Zhanqiang Fang*, Xiuqi Qiu, Jinhong Chen, Xinhong Qiu

*School of Chemistry and Environment, South China Normal University, Guangzhou 510006, Guangdong, China*

ARTICLE INFO

*Article history:*
Received 8 November 2009
Received in revised form 13 July 2010
Accepted 30 July 2010
Available online 6 August 2010

*Keywords:*
Nanoscale particles
Zero-valent metal
Metronidazole
Degradation
Steel pickling waste liquor

ABSTRACT

In this study, steel pickling waste liquor was employed to obtain reactive nanoscale zero-valent metal (nZVM) with the purpose of engineering application. The degradation of metronidazole reacted with as-prepared nZVM in water was investigated to explore the feasibility of using the nZVM to treat antibiotics in wastewater. The synthesized nZVM was characterized by Brunauer–Emmett–Teller (BET) surface analyzer, transmission electron microscopy (TEM), scanning electron microscopy (SEM), X-ray diffraction (XRD), X-ray photoelectron spectroscopy (XPS) and energy dispersive X-ray spectrometer (EDS). The results showed that the nZVM (20–40 nm) with crystalline structure had a BET surface area of 35 $m^2/g$. XPS and EDS only detected Fe, C and O on the surface, suggesting Ni and Zn distributed inside the core of nanoscale alloy. Degradation of metronidazole followed the pseudo-first-order kinetics, and the observed reaction rate constant ($k_{obs}$) could be improved with increasing nZVM dosage, as well as with diminishing initial metronidazole concentration and pH. A high reaction rate was observed at reduction potential, indicating that electrons and hydrogen species produced by nZVM were driving forces of reaction. The surface area-normalized rate coefficient ($k_{SA}$) for nZVM (0.254 $L\,min^{-1}\,m^{-2}$) was 375.2 times larger than that for commercial iron powder ($6.67 \times 10^{-4}$ $L\,min^{-1}\,m^{-2}$). Several possible pathways of degradation of metronidazole were proposed according to the results of UV–vis spectra and HPLC chromatograms.


## 1. Introduction

Nanotechnology has been successfully applied in the field of pollution abatement to remove of toxic contaminants, remediate of groundwater, etc. [1–3]. Due to their high specific surface area, environmental benignity and capabilities as catalytic degradation of contaminants through changing reaction mechanism [4–6], nanoscale zero-valent iron (nZVI) and iron-based metallic (bimetal or trimetal) nanoparticles (nZVM) are deemed to be promising nanomaterials, which have gained much attention for persistent pollutant treatment. Recently, many researches on degradation of toxic contaminants, including chlorinated organic substances [7], nitrate [8], azo dye [9], nitrobenzene [10], and heavy metal [11,12], have been reported. Undoubtedly, nZVI or nZVM will be commercially used to degrade persistent toxic substances (PTS) in the future.

Researchers have recently developed two kinds of methods to prepare nanoparticles, including physical methods (e.g., inert gas condensation, high-energy ball milling) and chemical methods (e.g., liquid-phase reduction, reverse micelle) [13]. Liquid-phase reduction method is widely used for its simplicity and productivity. In this method, borohydride reduces iron ions to nZVI. Additionally, nano-iron-based metallic systems are created by reductive deposition of other metal ions on the nZVI surface [3,14]. However, many chemicals (e.g., borohydride, metal salts) are consumed during the preparation, resulting in high production cost which limits the engineering application of nZVM. On the other hand, pickling waste liquor discharged from steel industry during pickling process is highly attractive and reclaimable resource with many iron and nickel ions, whose contents are up to 122 g/L and 17 mg/L, respectively. This by-product could be used to prepare nZVM. However, much of pickling waste liquor in China is directly discharged into the watershed, leading to severe environmental pollution and waste of a potential resource. Although many possible applications of nZVM have been reported, the feasibility of preparing nZVM by utilizing steel pickling waste liquor to decrease the production cost has not been demonstrated.

Nowadays, pharmaceutical and personal care products (PPCPs) have been listed as priority substances by European Union Water Framework Directive (EUWFD), and they routinely exist in cosmetics, domestic products and especially in pharmaceutical products such as antibiotics, beta-blockers, antiseptics, antiepileptics and anti-inflammatories [15]. Antibiotics are environmentally called "pseudo-persistent compounds" [16] for their toxicity, undegra-

* Corresponding author. Tel.: +86 20 39310250, fax: +86 20 39310187.
*E-mail address:* zhqfang@scnu.edu.cn (Z. Fang).

0926-3373/$ – see front matter © 2010 Elsevier B.V. All rights reserved.
doi:10.1016/j.apcatb.2010.07.035

dation and causing drug-resistant [17]. Currently, more than 100 kinds of antibiotics are produced in China, being the top of the worldwide yield. The occurrence of antibiotic residues in the sewage sludge and river sediment of Guangzhou, South China ranges from 6.8 to 125.6 ng/g dry weight [17]. Antibiotics are also found in surface water, ground water and soil, whose concentration levels are ranged from 20 to 32,000 ng/L, 240 to 410 ng/L and 0.5 to 900 ng/g, respectively [18]. Metronidazole with methyl and nitro that belongs to nitroimidazole is a common antibiotic drug, which is abused for treating infections, and its maximum concentrations detected in effluent of hospital and sewage treatment plant are 9400 and 127 ng/L, respectively [19,20]. Because of its high solubility (7.02 g/L, in water, 298 K), refractory and suspected carcinogenesis [21], metronidazole must be completely eliminated from the effluent of wastewater treatment plant before discharging. Nevertheless, conventional treatment systems based on microbial methods have been unable to remove this type of organic compound due to its complex molecular structure [22]. So far, studies of metronidazole removal by advanced oxidation process [23] have been reported. However, degradation of metronidazole using nZVI or nZVM has not been undertaken.

The major objectives of this work are: (1) to prepare nZVM from steel pickling waste liquor and to characterize its properties; (2) to degrade antibiotic metronidazole by the obtained nZVM.

## 2. Experimental

### 2.1. Materials

Sodium borohydride ($NaBH_4$), polyvinylpyrrolidone (PVP K-30) and ethanol (Analytical Reagent) were purchased from Tianjin Damao Chemical Reagent Factory (China); metronidazole (Analytical Reagent) was obtained from Guangzhou Chemical Factory (China); acetonitrile (HPLC grade) was from Merck (German). Metronidazole standard ($C_6H_9N_3O_3$) used for establishing standard curve was obtained from Pharmaceutical and Biological Products Testing Institute of China.

Pickling waste liquor obtained from Jinlai steel plant in Guangzhou (China) was diluted or adjusted to desired pH value by hydrochloric acid or sodium hydroxide solution before use. Commercial iron powder (ZVI) with an average diameter of 69 μm and a specific surface area of 3 $m^2$/g was purchased from Tianjin Kermel Chemical Reagent Co. Ltd. (China). It was soaked in hydrochloric acid solution (5 mol/L) for 10 min, then washed by deionized water and dried in vacuum box just prior to reaction.

### 2.2. Preparation of nanoparticles

Nanoparticles were synthesized by modifying the method described by Song and Carraway [3], since there were $Fe^{2+}$ and $Fe^{3+}$ ions existing in the waste liquor, nZVM was synthesized according to the following reactions [24,25]:

$$Fe(H_2O)_6{}^{2+} + 2BH_4{}^- \rightarrow Fe^0\downarrow + 2B(OH)_3 + 7H_2\uparrow \quad (1)$$

$$Fe(H_2O)_6{}^{3+} + 3BH_4{}^- + 3H_2O \rightarrow Fe^0\downarrow + 2B(OH)_3 + 10.5H_2\uparrow \quad (2)$$

The diluted pickling waste liquor was treated with aqueous sodium borohydride solution in the presence of sodium hydroxide as pH stabilizer. In a typical experiment, diluted pickling waste liquor (5 mL, $c_{Fe}$ = 0.1 mol/L) and polyvinylpyrrolidone (0.5 g) reacting as dispersant were prepared in a 500 mL three-necked flask. Before the reaction, the deionized water was bubbled with nitrogen gas for 30 min to remove dissolved oxygen. The nanoparticles were synthesized by dropwise addition of sodium borohydride solution into the flask simultaneously with electric stirring. Nanoparticles were then washed by water 3 times, and rinsed by ethanol 3 times. Finally, the nanoparticles were collected and stored in ethanol or vacuum box for subsequent experiments. The production cost of reusable nZVM was calculated to be $0.49/g according to the market price of analytical grade reagents (calculation procedure not shown).

Nanoscale $Fe^0$, nanoscale $Ni^0$ and ZnO were prepared from chemicals ($FeSO_4$, $NiCl_2$, $ZnSO_4$, etc.) using the same method as preparing for nZVM. The synthesized nanoparticles were dried and stored in vacuum box.

### 2.3. Characterization of nanoparticles

The concentrations of metallic elements in raw waste liquor were acquired by ICP-AES (IRIS Intrepid || XSP, Thermo Elemental Company, USA). The synthesized nZVM was digested using chemical solution method recommended by US Environmental Protection Agency (US EPA 3050B), followed by the analysis of contents of Fe, Ni and Zn in nZVM. The concentrations of anions in raw waste liquor were measured by ion chromatography (DX-600, Dionex, USA). The chromaticity of steel pickling waste liquor was determined by dilution multiple method. The concentration of hydrogen ion was obtained using pH meter.

The measurement of specific surface area of nZVM was performed using nitrogen adsorption isotherm by specific surface area analyzer (ASAP2020M, Micromeritics Instrument Corp., USA). The surface, morphology and size of nZVM were viewed with SEM (XL-30ESEM, PHILIPS, Netherland) and TEM (TECNAI 10, PHILIPS, Netherland). The crystal structures of as-prepared nanoparticles were examined by XRD (Y-2000, Dandong Aolong ray Instrument Co. Ltd., China) with Cu Kα radiation. Element composition of nZVM was determined by XPS (ESCALAB 250, Thermo-VG Scientific, USA) and EDS (ISIS-300, Oxford, UK).

### 2.4. Experimental procedures

The batch experiments of metronidazole degradation were performed in a 500 mL three-necked flat-bottomed flask, into which the as-prepared nZVM was introduced. After that, metronidazole aqueous solution (300 mL) was added and stirred under nitrogen flow and periodically sampled by plastic syringe. The sample was filtered immediately through 0.45 μm membrane filters for HPLC analysis. At the end of the reaction, the samples accounted for less than 5% of the volume of solution. Thus, opposite impacts of the changes of the volume was negligible. The benchmark experiment conditions were: temperature, 25 ± 1 °C; initial pH, 5.60; initial metronidazole concentration, 80 mg/L; nZVM dosage (fresh sample), 0.100 g/L; speed of stirring,150 rpm; nitrogen flow, 100 mL/min. Condition experiments were conducted under the benchmark experiment conditions except for the changes in corresponding conditions.

### 2.5. Analytical methods

The as-prepared nanoscale zero-valent metal (nZVM) was digested by chemical solution method. Firstly, concentrated hydrochloric acid (10 mL) was added into a porcelain crucible containing nZVM, and the crucible was placed on a hot plate till the nZVM was completely digested. Secondly, the solution in the crucible was transferred into a 100 mL measuring flask and brought to volume by deionized water.

Metronidazole concentrations were measured by high performance liquid chromatography (HLPC, Shimadzu, Japan) equipped with a UV detector (SPD-10AV) and a C18 column (250 mm × 4.6 mm). Mobile phase: 20% acetonitrile and 80% water; flow rate: 1.0 mL/min; injection volume: 20 μL; absorbance detection: 318 nm.

**Table 1**
Physical and chemical characteristics of steel pickling waste liquor.

| Item | Waste liquor |
|---|---|
| Color | Brown-yellow |
| Chromaticity (fold) | 1250 |
| $H^+$ (mg/L) | 910 |
| Fe (mg/L) | 121,860 |
| Ni (mg/L) | 17 |
| Zn (mg/L) | 3 |
| $Cl^-$ (mg/L) | 216,400 |
| $SO_4^{2-}$ (mg/L) | 1050 |
| $NO_3^-$ (mg/L) | 850 |

### 2.6. Kinetics analysis

The degradation of metronidazole in a batch system was explained by a pseudo-first-order equation [5]:

$$\ln(c_t/c_0) = -k_{obs}t \quad (3)$$

where $c_t$ is the concentration of metronidazole at selected times (mg/L); $c_0$ is the initial metronidazole concentration (mg/L); $k_{obs}$ is the observed rate constant ($min^{-1}$); and $t$ is time (min).

The observed reaction rate constant ($k_{obs}$) values were calculated by the method of linear regression. The surface area-normalized rate coefficient ($k_{SA}$) was then obtained using the following equation:

$$k_{obs} = k_{SA} a_s \rho_m \quad (4)$$

where $a_s$ is the specific surface area ($m^2/g$), and $\rho_m$ is the particles dosage (g/L).

## 3. Results and discussion

### 3.1. Nanoscale zero-valent metal characterization

The main physical characteristics and chemical composition of steel pickling waste liquor are shown in Table 1. ICP analysis indicated that the contents of Fe, Ni and Zn in steel pickling waste liquor were 121,860, 17 and 3 mg/L, respectively. The ratios of Fe, Ni and Zn in the synthesized nZVM after digested and analyzed were 99.987%, 0.011% and 0.002%, respectively.

The morphology and size of synthesized nZVM were shown in TEM images (Fig. 1a). The images showed that nZVM (black dot) was covered by a layer of iron oxide (grey surface), demonstrating that nZVM was core–shell structure with particle size in a range of 20–40 nm, which corresponded to the nZVI prepared using chemicals [25,26]. The spherical nanoparticles formed a chainlike, aggregated structure because of magnetic interactions between the nanoparticles and a natural tendency to remain in more thermodynamically stable state [27]. As shown in SEM images of nZVM (Fig. 1b), nanoparticles were observed to be roughly spherical and structurally defective on the surface, suggesting that numerous reactive sites could be provided by nZVM. The synthesized samples were dried in vacuum box at temperature of 50 °C before the determination of specific surface area. It was found that the nZVM had a typical BET surface area of 35 $m^2/g$, which was similar to other researches [26,28,29]. Specific surface area was an important property which influenced the activity of the nZVM and the kinetics of reaction. Compared to commercial ZVI, nZVM was much smaller in diameter and higher in BET surface area, which made it attractive for eliminating contaminants.

XPS and EDS were further used to study the surface chemical compositions of nZVM. As shown in Fig. 2a, XPS and EDS analyses revealed that Fe, C and O were present on the surface of nZVM. It could be deduced that: (1) little residual ethanol was existed on the surface; (2) nZVI was easily attacked by O when it was exposed to air. XPS and EDS also did not detect the presences of Ni and Zn on the surface of nanoparticles, suggesting that Ni and Zn distributed inside the core of nZVM or their loadings might be too low to be detected. Nevertheless, contents of Ni (0.011%) and Zn (0.002%) in solid nZVM were detected by ICP, so they were deemed to be deposited in nZVM [9,11]. As the interfacial reaction dominated the reaction process of nanoparticles, this kind of alloy nanoparticles could avoid the possible toxicity of the nickel ion released from nZVM.

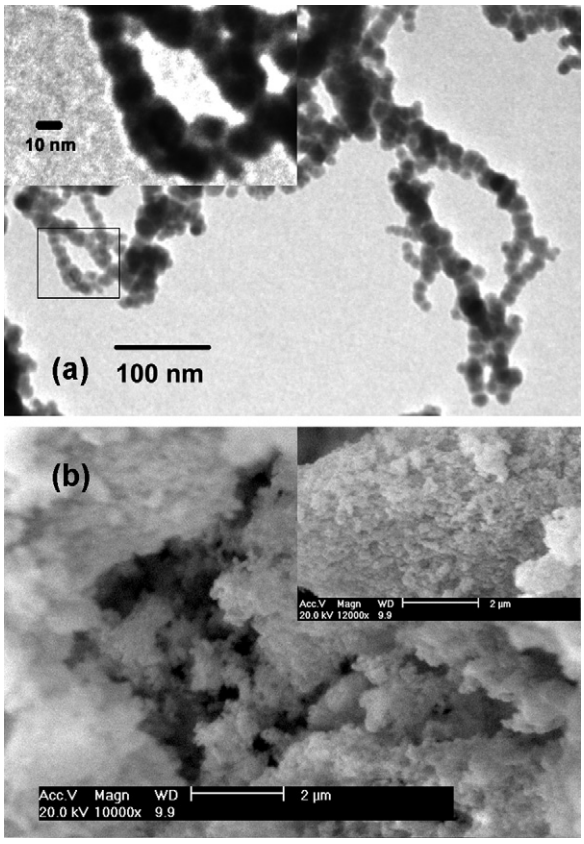


**Fig. 1.** (a) Different scale TEM images of nZVM and (b) different scale SEM images of nZVM.

The XPS spectra of Fe (2p) in Fig. 2b showed three peaks at the binding energies of 706.9, 710.8 and 725.1 eV. Peak at 706.9 eV demonstrated the existence of nZVI, while broad peaks at 710.8 and 725.1 eV were attributed to iron oxides ($\alpha$-$Fe_2O_3$), indicating that the surface of nZVM was also covered by iron oxide film which might form during preparation or analysis process. This kind of core–shell structure was consistent with the observation previously obtained by TEM.

X-ray powder diffraction analysis (Fig. 3a) showed that the most prominent diffraction peaks at $2\theta = 44.72°$, 65.08° and 82.40° could be indexed as those of $Fe^0$ corresponding to the (1 1 0), (2 0 0) and (2 1 1) planes, respectively. The remarkable peaks revealed that nZVM prepared from waste liquor were highly crystalline [2]. Its structure was quite different from the nZVI prepared from chemicals as reported by Wang et al. [30]. It was believed that nanoscale iron formed amorphous alloy with a number of structural defects on the surface and hydrogen concentration increased when it was exposed to water [31]. The latter, in fact, was considered to be the first step of catalytic degradation. As shown in Fig. 3(b–d), the morphology of nanoparticles prepared from chemicals ($FeSO_4$, $NiCl_2$, $ZnSO_4$, etc.) were all irregular and amorphous. For instance, nZVI (b) based on a broad peak from 44° to 45° $2\theta$ was acknowledged for $\alpha$-$Fe^0$. The results also indicated that Ni (c) existed in the form

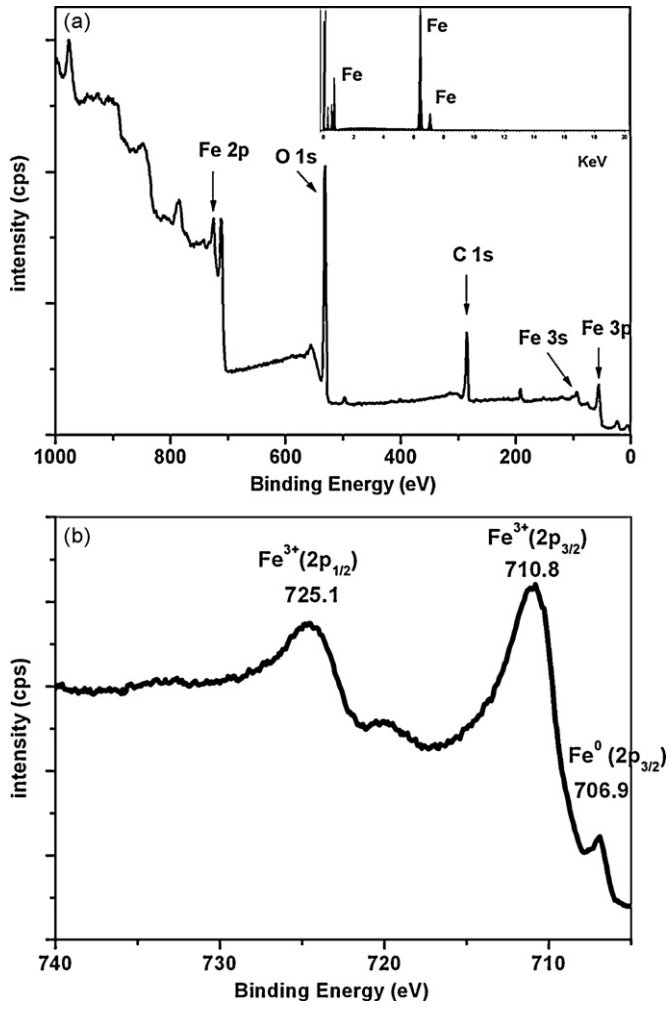


**Fig. 2.** (a) XPS and EDS (inset) spectra of nZVM and (b) XPS spectrum for the narrow scan of Fe (2p) on the surface of nZVM.

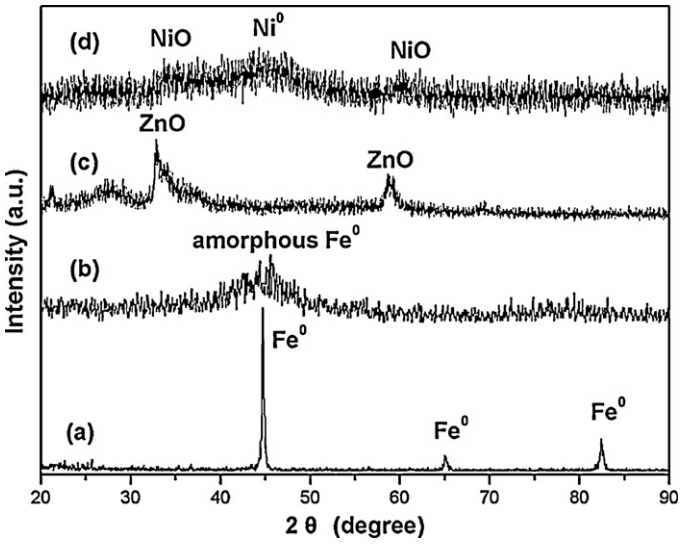


**Fig. 3.** XRD patterns of nZVM (a), nZVI (b), nano-ZnO (c) and nano-Ni (d).

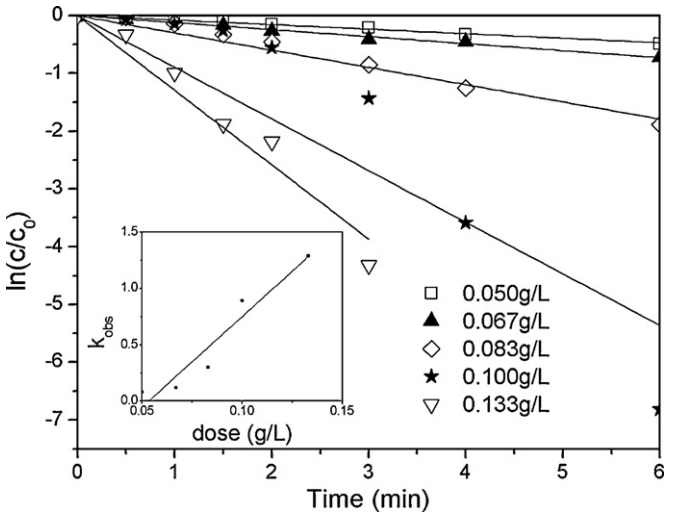


**Fig. 4.** Effect of nZVM dosage on the degradation of metronidazole. Inset: correlation of the observed rate constant ($k_{obs}$) and nZVM dosage.

of elementary substances with oxides on the surface, while Zn (d) was expected for ZnO after the reduction of sodium borohydride.

### 3.2. Effect of nZVM dosage on metronidazole degradation

The effect of different nZVM dosages (0, 0.050, 0.067, 0.083, 0.100 and 0.133 g/L) on the reaction rate was studied (Fig. 4). The extra effects of agitation, light and bubbling on metronidazole reduction were found to be insignificant. In contrast, the increase of nZVM dosage greatly enhanced the degradation efficiency, since the reaction occurred on the surface of nZVM and the available surface area, adsorption and reaction sites increased with increasing concentration of nanoparticles [7,32]. About 99% of degradation efficiency was achieved within 6 min when the doses were 0.100 and 0.133 g/L. The nZVM presented extremely great capability of catalytic degradation because of its small diameter and huge surface area, which had been earlier demonstrated by TEM and BET. Based on these results, the optimum dosage of nZVM in the level of 0.100 g/L was chosen for subsequent metronidazole degradation.

The inset in Fig. 4 shows the plot of the pseudo-first-order rate constant for metronidazole removal versus nZVM dosage. It shows that the rate constant ($k_{obs}$) increased linearly with increasing dose. However, the slightly flattening of the curve at lower dose perhaps was due to insufficient mixing during the reaction. The kinetic data under the selected dosages of nZVM were listed in Table 2. For instance, the surface area-normalized rate coefficient ($k_{SA}$) for nZVM ranged from 0.046 to 0.277 L min$^{-1}$ m$^{-2}$ when the

**Table 2**
The kinetic data under different experimental conditions.

| Dose (g/L) | $C_0$ (mg/L) | Initial pH | $k_{obs}$ (min$^{-1}$) | $k_{SA}$ (L min$^{-1}$ m$^{-2}$) | $R^2$ |
|---|---|---|---|---|---|
| 0.050 | 80 | 5.60 | 0.08 | 0.046 | 0.99 |
| 0.067 | 80 | 5.60 | 0.12 | 0.051 | 0.99 |
| 0.083 | 80 | 5.60 | 0.30 | 0.103 | 0.98 |
| 0.100 | 80 | 5.60 | 0.89 | 0.254 | 0.87 |
| 0.133 | 80 | 5.60 | 1.29 | 0.277 | 0.98 |
| 0.100 | 45 | 5.60 | 1.08 | 0.309 | 0.97 |
| 0.100 | 60 | 5.60 | 0.98 | 0.280 | 0.93 |
| 0.100 | 100 | 5.60 | 0.65 | 0.186 | 0.90 |
| 0.100 | 120 | 5.60 | 0.11 | 0.031 | 0.93 |
| 0.100 | 80 | 2.03 | 2.42 | 0.691 | 0.96 |
| 0.100 | 80 | 4.00 | 1.15 | 0.329 | 0.98 |
| 0.100 | 80 | 7.03 | 0.46 | 0.131 | 0.86 |
| 0.100 | 80 | 9.04 | 0.20 | 0.057 | 0.95 |

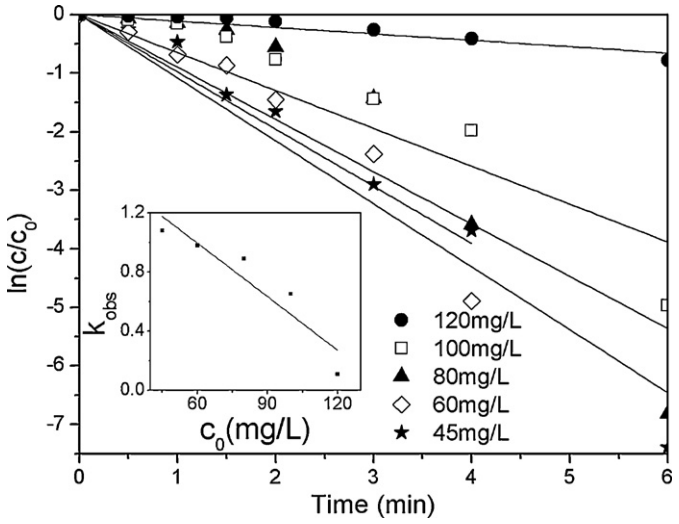


**Fig. 5.** Effect of initial metronidazole concentration on the degradation. Inset: correlation of $k_{obs}$ and initial metronidazole concentration.

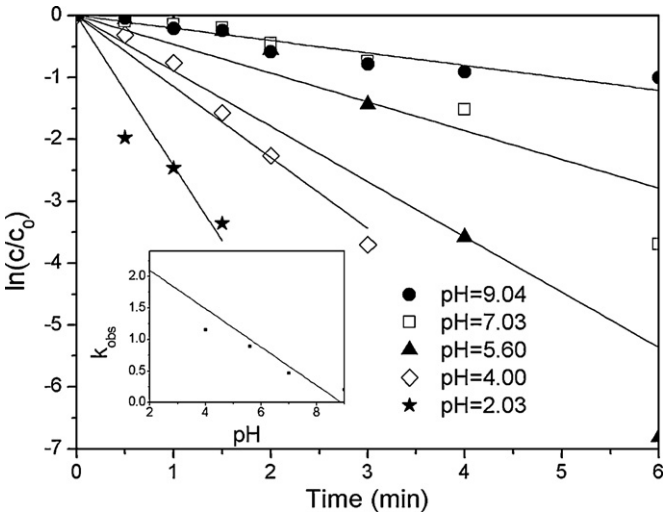


**Fig. 6.** Effect of pH on the degradation of metronidazole. Inset: correlation of $k_{obs}$ and initial pH.

dose changed in the range of 0.050–0.133 g/L under the benchmark experiment conditions.

### 3.3. Effect of initial metronidazole concentration on metronidazole degradation

Adsorption-, surface-reaction-, or desorption-limited kinetics could be further confirmed by investigating the variability of $k_{obs}$ with initial concentration [33]. The effect of initial metronidazole concentration on the reaction rate was evaluated using various initial concentrations (Fig. 5). Metronidazole at initial concentration of 45, 60, 80 and 100 mg/L almost disappeared within 6 min, while the reductive rate retained slow state and the removal efficiency only reached 46% throughout the reaction when the initial concentration was 120 mg/L. The active surface sites offered by nZVM for the reaction were restricted by increasing metronidazole concentration. The inset in Fig. 5 shows the correlation between $k_{obs}$ and the initial concentration of metronidazole. The results presented in the figure indicated that $k_{obs}$ decreased linearly up to 100 mg/L of initial metronidazole concentration, with slight deviation at the highest concentration (120 mg/L), indicating that metronidazole transformations were surface-reaction limited kinetic domain over the concentration range of 45–120 mg/L. It was believed that the metronidazole degradation by nZVM was a heterogeneous reaction process including adsorption and surface-reaction processes. Increasing initial metronidazole concentration could enhance the adsorption of metronidazole by nZVM, but might lead to the package of nanoparticles by metronidazole, which blocked their further contact and prevented the continuous generation of hydrogen. It was observed that ratio of nZVM to metronidazole should be kept above 1:1 in order to preserve a high degradation rate.

The kinetic data under the selected initial concentrations of metronidazole for were summarized in Table 2.

### 3.4. Effect of initial pH on metronidazole degradation

The pH value was known to have a significant effect on the degradation process of organic contaminants with nZVM, for it greatly affected the corrosion of nZVM serving as an adsorption catalyst [34], producing more reactive sites at lower pH and more passivation by oxide or hydroxide at higher pH. Nonetheless, rapid corrosion of nZVM at too low pH (<2) also leaded to insufficient degradation [35].

To investigate the interaction of these effects, degradation of metronidazole was examined at a series of pH values. In this study, metronidazole solution was adjusted to different initial pH values (2.03, 4.00, 5.60, 7.03 and 9.04) by diluted sulfuric acid or sodium hydroxide, without pH adjusting during the reaction. The degradation efficiencies were up to at least 97% within 6 min when initial pH ranged from 2.03 to 7.03, while the efficiency only reached 63% at initial pH of 9.04, indicating that passivation weakened the degradation capability of nZVM instead of depriving at alkaline condition [35].

As shown in Table 2, the observed rate constants were 0.691–0.057 $min^{-1}$, respectively, at pH 2.03–9.04. Obviously, lower initial solution pH value resulted in much faster degradation of metronidazole by nZVM. Fig. 6 shows that the degradation followed pseudo-first-order kinetics at a given pH value. The results also indicated that reaction rate remarkably increased with diminishing pH (inset of Fig. 6). This effect was ascribed to the fact at low pH value that: (1) the oxides on the surfaces of nanoparticles were promptly dissolved and the active sites were unlocked; (2) iron corrosion producing abundant hydrogen for hydrogenation reaction was accelerated [36]. However, nZVM would be exhausted after substantial corrosion, leading to insignificant degradation in the subsequent reaction. Moreover, the mass balance of Fe in solid and liquor phases was also examined. The results showed that most of Fe existed in solid phase and the dissolved Fe was very low in content (maximum dissolved rate of Fe was 0.69% at initial pH 5.60) throughout the reaction. The surface reactions might be described as follows [36]:

$$Fe^0 + 2H_2O \rightarrow Fe^{2+} + H_2 + 2OH^- \quad (5)$$

$$Fe^0 + 2H^+ \rightarrow Fe^{2+} + 2e^- \quad (6)$$

$$2H^+ + 2e^- \rightarrow H_2\uparrow \quad (7)$$

$$H^+ + e^- \xrightarrow{Ni} H^\bullet \quad (8)$$

### 3.5. Comparison of metronidazole degradation at different potentials

Reactions were conducted under reduction potential (bubbling $N_2$ at a flow rate of 100 mL/min) and oxidation potential (bubbling air at a flow rate of 400 mL/min), respectively, at pH 5.60, at initial metronidazole concentration of 60–100 mg/L and nanoscale dose of 0.1 g/L. The results indicated that, at initial concentration

**Table 3**
The kinetic data at different potentials and initial metronidazole concentrations.

| $C_0$ (mg/L) | Reduction potential | | | Oxidation potential | | |
|---|---|---|---|---|---|---|
| | $k_{obs}$ ($min^{-1}$) | $k_{SA}$ ($L\,min^{-1}\,m^{-2}$) | $R^2$ | $k_{obs}$ ($min^{-1}$) | $k_{SA}$ ($L\,min^{-1}\,m^{-2}$) | $R^2$ |
| 60 | 0.92 | 0.263 | 0.96 | 0.57 | 0.163 | 0.89 |
| 80 | 0.89 | 0.254 | 0.87 | 0.46 | 0.131 | 0.96 |
| 100 | 0.64 | 0.183 | 0.90 | 0.29 | 0.083 | 0.98 |

of 100 mg/L, removal efficiency reached 84% at oxidation potential, while over 99% of metronidazole disappeared at reduction potential.

As shown in Table 3, $k_{obs}$ at reduction potential were 0.64–0.92 and 0.29–0.57 $min^{-1}$ at oxidation potential, respectively. Fig. 7 shows the comparison of $k_{obs}$ at different potentials under the benchmark experiment conditions. The results indicated that $k_{obs}$ at reduction potential were higher than those at oxidation potential, demonstrating that reduction potential preserved the high activity of nZVM [37], and dissolved oxygen weakened the degradation capability of nZVM. The dissolved oxygen served as an electron acceptor, which exhausted electrons produced by nZVM [38]. Besides, dissolved oxygen rapidly attacks the nZVM, and iron hydroxides or oxides hindering the subsequent reaction were formed on the surface.

### 3.6. Comparison of metronidazole degradation by ZVI, nZVI and nZVM

The degradations by commercial ZVI, nZVI and nZVM were performed under the benchmark experiment conditions, and comparison of degradation efficiencies by various materials are shown in Fig. 8. The results indicated that ZVI could not effectively eliminate metronidazole and reaction rate changed insignificantly with increasing ZVI dosage. In contrast, increasing dosage of nanoparticles dramatically enhanced the reaction rate, suggesting that the reaction activity of nanoparticles was much higher than that of ZVI.

Compared to ZVI and nZVI prepared from chemicals ($FeSO_4$, etc.), $k_{SA}$ for nZVM (0.254 $L\,min^{-1}\,m^{-2}$) was 375.2-fold and 0.65-fold than that for ZVI ($6.67\times10^{-4}$ $L\,min^{-1}\,m^{-2}$) and nZVI (0.39 $L\,min^{-1}\,m^{-2}$), respectively, when particles dosage was 0.1 g/L, initial concentration of metronidazole was 80 mg/L and initial pH was 5.60. The $k_{SA}$ for ZVI at dose of 1.17 g/L with the same specific surface area of nZVM at dose of 0.1 g/L was 0.043 $L\,min^{-1}\,m^{-2}$, which was still much smaller than $k_{SA}$ for nZVM (0.254 $L\,min^{-1}\,m^{-2}$) and $k_{SA}$ for nZVI (0.39 $L\,min^{-1}\,m^{-2}$). Since the reaction initiated by ZVI was surface-mediated [39,40], high metronidazole concentration would saturate the surface reactive sites of ZVI, leading to low reaction rate and a transition to zero-order kinetics [33]. More reactive sites could be obtained by nanoparticles for their higher specific surface area, which significantly intensified the removal rate of metronidazole.

In the case of nZVM and nZVI, $k_{SA}$ for nZVI (0.39 $L\,min^{-1}\,m^{-2}$) was 1.5 times larger than that for nZVM (0.254 $L\,min^{-1}\,m^{-2}$) under the benchmark experiment conditions, indicating that the grade of raw material, such as industrial grade and analytical grade, impacted the quality of nanoparticles. Compared to ZVI, the relatively small disparity between both nanoparticles demonstrated the availability of nZVM prepared from steel pickling waste liquor.

### 3.7. Comparison of metronidazole degradation using dried nZVM, nZVI, nanoscale $Ni^0$ and nanoscale ZnO

To investigate the percentage of reduction of metronidazole due to nano-$Fe^0$, nano-$Ni^0$ and nano-ZnO, the degradation of metronidazole by dried nZVM, nZVI, nano-$Ni^0$ and nano-ZnO were carried out under the following experiment conditions: temperature, 25 ± 1 °C; initial pH, 5.60; solution volume, 100 mL; initial metronidazole concentration, 80 mg/L; nZVM, nZVI, nano-$Ni^0$ and nano-ZnO dosages (dried sample), 0.3 g/L; speed of stirring, 150 rpm.

As shown in Fig. 9, removal efficiencies of metronidazole by dried nano-$Ni^0$, dried nano-ZnO, dried nZVI and dried nZVM were 5.1%, 6.7%, 55.9% and 52.5%, respectively, within 90 min. The results indicated that dried nano-$Ni^0$ and dried nano-ZnO could not effectively remove metronidazole, while dried nZVI and nZVM exhibited similar removal capacity. As previously calculation, the ratios of Fe, Ni and Zn in solid nZVM were 99.987%, 0.011% and 0.002%,

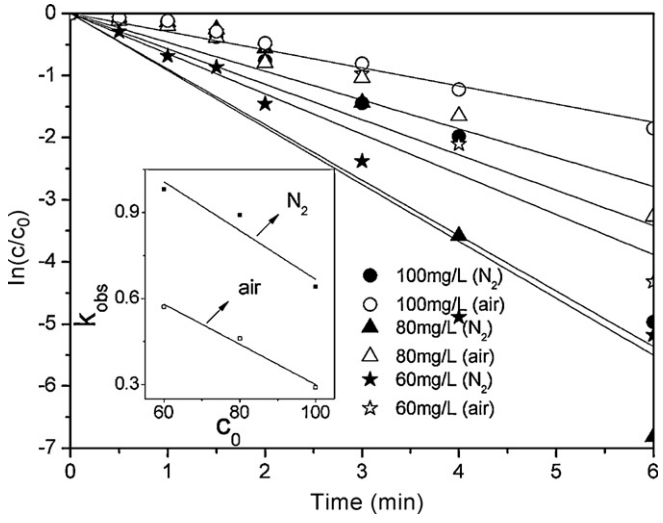


**Fig. 7.** Comparison of metronidazole degradation at different potentials. Inset: correlation of $k_{obs}$ and initial metronidazole concentration under different potentials. ●, ▲, ★ reduction potential. ○, △, ☆ oxidation potential.

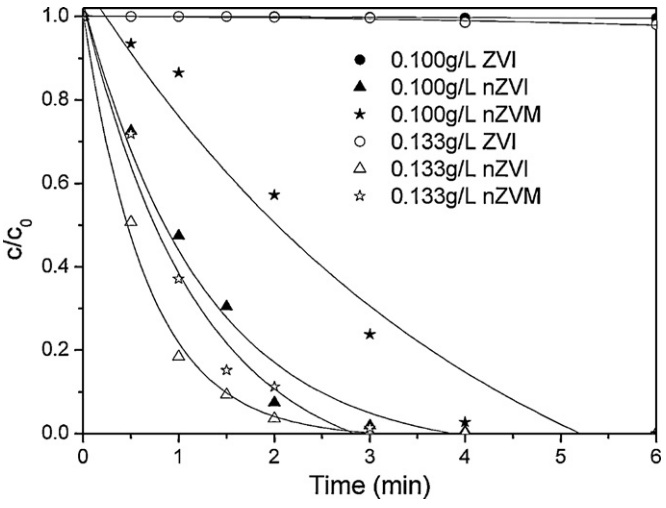


**Fig. 8.** Comparison of metronidazole degradation by ZVI, nZVI and nZVM. Variable: dosages of commercial ZVI, nZVI and nZVM.

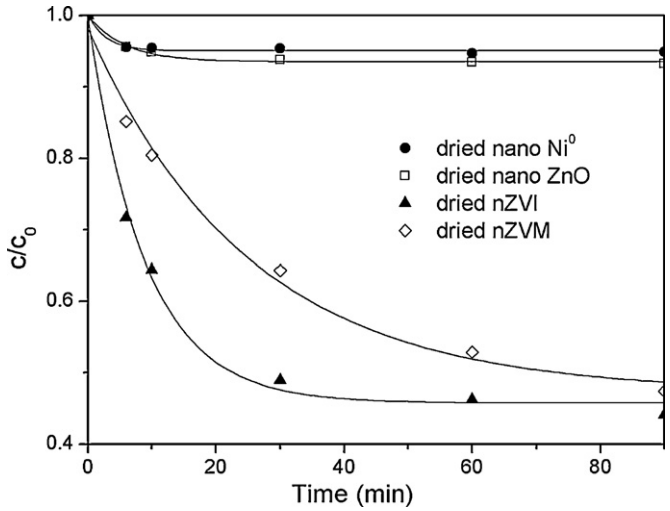


**Fig. 9.** Comparison of metronidazole degradation using dried samples. Variable: dried nanoscale $Ni^0$, dried nano-ZnO, dried nZVI and dried nZVM.

respectively. The ratios of Ni and Zn were very low, and the respective removal capacities of Ni and Zn were much weaker than that of Fe. Consequently, the vast majority of reduction of metronidazole was due to $Fe^0$, the removal percentage due to respective Ni and Zn accounted for little (Ni: 0.1%; ZnO: 0.03%, calculation not shown). Although the function of Ni acted as catalysis was crucial for the reductive degradation [9], removal rate for dried nZVM was observed to be slightly smaller than that for dried nZVI. This difference might be due to that the industrial grade of the steel pickling waste liquor, whose complicated chemical composition might more or less influence the property of nZVM.

### 3.8. Transformation of metronidazole by nZVM

The UV–vis spectra of metronidazole degradation at different reacting times by nZVM are presented in Fig. 10. Several observations were summarized for the reaction based on the spectral profile transitions: (1) the characteristics absorption band of metronidazole was around 318 nm, which quickly disappeared within 4 min; (2) gradual increase of absorbance between 200 and 240 nm demonstrated the formation of intermediate and final products; (3) low levels of absorbance spectrum at 6 min were due

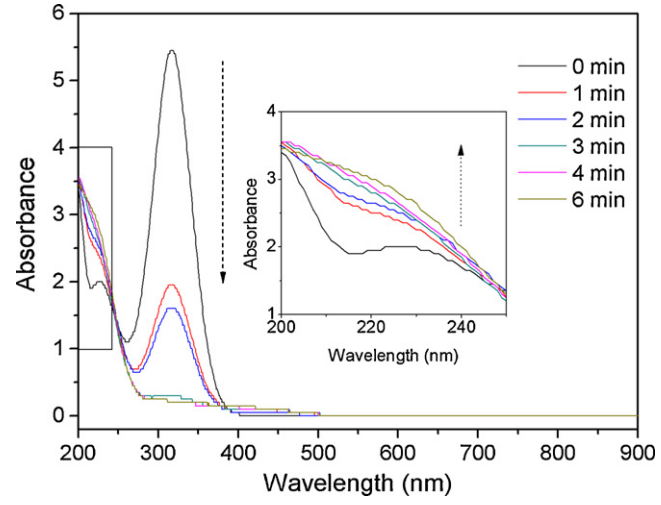


**Fig. 10.** Variation of UV–vis spectrum of metronidazole with reaction time under the benchmark experiment conditions.

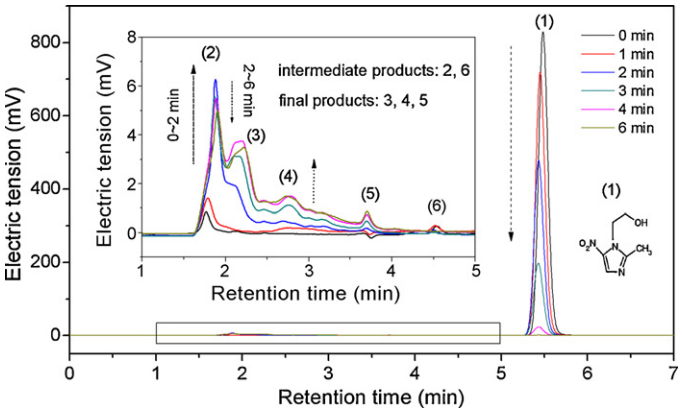


**Fig. 11.** Variation of HPLC chromatogram of metronidazole with reaction time under the benchmark experiment conditions.

the disappearance of characteristic absorption functional groups of metronidazole.

Fig. 11 illustrates the HPLC chromatograms of metronidazole solution at varied reaction times. Metronidazole (NO. 1 peak) eluted at retention time of 5.3 min rapidly disappeared, and was substituted for intermediate products and final products. All the by-products were eluted from the chromatographic column before metronidazole. As shown in the chromatograms of intermediate products of metronidazole (inset in Fig. 11), five chromatographic peaks were observed at the retention time of 1.7–4.5 min, although several peaks were not well separated. The NO. 2 and NO. 6 peaks representing intermediate products increased in the first 2 min, while decreased after 2 min. The other peaks increased all the while, indicating that other peaks stood for final products. The by-products exhibited low level of emission signals, which were in accordance with those previously observed in UV–vis spectra, suggesting the disappearance of characteristic absorption functional groups of metronidazole.

According to the results of UV–vis spectra and HPLC chromatograms, plausible degradation pathways were adsorption on the surface of nZVM, followed by nitro reduction, hydroxyethyl cleavage or N-denitration involving the electrons and hydrogen species produced by nZVM [41,42]. Possible intermediate products of metronidazole {1-(2-hydroxyethyl)-2-methyl-5-nitroimidazole} were inferred and outlined in Fig. 12, involving multiple intermediate products like 1-(2-hydroxyethyl)-2-

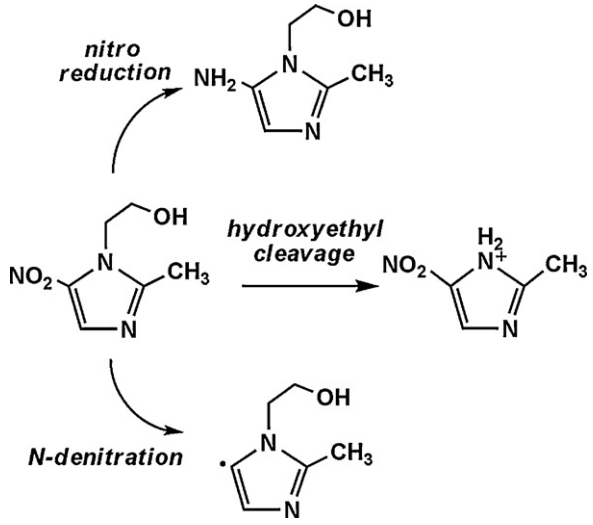


**Fig. 12.** Possible pathways of metronidazole degradation.

methyl-5-aminooimidazole, 2-methyl-5-nitroimidazole, or 1-(2-hydroxyethyl)-2-methyl-5-imidazole. However, liquid chromatography–mass spectrometry (LC–MS) was suspected to be inaccurate to examine the intermediate products. Gas chromatography–mass spectrometry (GC–MS) is essential to further investigation for the characterization of by-products and to better understanding of the degradation mechanism.

## 4. Conclusions

The results from batch studies demonstrated that nZVM prepared from pickling waste liquor can effectively degrade metronidazole. The degradation was found to follow pseudo-first order kinetics and $k_{obs}$ was proportional to nanoparticles dosage and inversely proportional to initial metronidazole concentration and initial pH. Reduction potential was favorable for high activity of the nZVM, suggesting that iron oxide served as a negative character in the reaction. The reaction rate of metronidazole by nZVM ($k_{SA} = 0.254\ L\ min^{-1}\ m^{-2}$) was much higher than that for commercial ZVI ($k_{SA} = 6.67 \times 10^{-4}\ L\ min^{-1}\ m^{-2}$). The results obtained in this study highlight the fact that nZVM transformed metronidazole via catalytic degradation. According to the results of UV–vis spectra and HPLC chromatograms, plausible degradation pathways involving the electrons and hydrogen species produced by nZVM were infered.

## Acknowledgments

The authors are grateful for the financial support provided by National Science and Technology major Projects of Water Pollution Control and Management of China (2008ZX07011).

## References

[1] X.Q. Li, W.X. Zhang, Langmuir 22 (2006) 4638–4642.
[2] S.R. Kanel, J.M. Greneche, H. Choi, Environmental Science & Technology 40 (2006) 2045–2050.
[3] H. Song, E.R. Carraway, Applied Catalysis B-Environmental 78 (2008) 53–60.
[4] F. He, D.Y. Zhao, Applied Catalysis B-Environmental 84 (2008) 533–540.
[5] X.Y. Wang, C. Chen, Y. Chang, H.L. Liu, Journal of Hazardous Materials 161 (2009) 815–823.
[6] H.L. Lien, W.X. Zhang, Applied Catalysis B-Environmental 77 (2007) 110–116.
[7] C.B. Wang, W.X. Zhang, Environmental Science & Technology 31 (1997) 2154–2156.
[8] S.S. Chen, H.D. Hsu, C.W. Li, Journal of Nanoparticle Research 6 (2004) 639–647.
[9] A.D. Bokare, R.C. Chikate, C.V. Rode, K.M. Paknikar, Applied Catalysis B-Environmental 79 (2008) 270–278.
[10] X. Zhang, Y.M. Lin, Z.L. Chen, Journal of Hazardous Materials 165 (2009) 923–927.
[11] S.M. Ponder, J.G. Darab, T.E. Mallouk, Environmental Science & Technology 34 (2000) 2564–2569.
[12] Y.H. Xu, D.Y. Zhao, Water Research 41 (2007) 2101–2108.
[13] L. Li, M.H. Fan, R.C. Brown, J.H. Van Leeuwen, J.J. Wang, W.H. Wang, Y.H. Song, P.Y. Zhang, Critical Reviews in Environmental Science and Technology 36 (2006) 405–431.
[14] R.A. Doong, Y.L. Lai, Chemosphere 64 (2006) 371–378.
[15] D. Bendz, N.A. Paxeus, T.R. Ginn, F.J. Loge, Journal of Hazardous Materials 122 (2005) 195–204.
[16] M.D. Hernando, M. Mezcua, A.R. Fernandez-Alba, D. Barcelo, Talanta 69 (2006) 334–342.
[17] C.M. Tang, Q.X. Huang, Y.Y. Yu, X.Z. Peng, Chinese Journal of Analytical Chemistry 37 (2009) 1119–1124.
[18] N. Kemper, Ecological Indicators 8 (2008) 1–13.
[19] M.J. Gomez, O. Malato, I. Ferrer, A. Aguera, A.R. Fernandez-Alba, Journal of Environmental Monitoring 9 (2007) 718–729.
[20] R. Rosal, A. Rodriguez, J.A. Perdigon-Melon, A. Petre, E. Garcia-Calvo, M.J. Gomez, A. Aguera, A.R. Fernandez-Alba, Water Research 44 (2010) 578–588.
[21] M. Sanchez-Polo, J. Lopez-Penalver, G. Prados-Joya, M.A. Ferro-Garcia, J. Rivera-Utrilla, Water Research 43 (2009) 4028–4036.
[22] M. Sanchez-Polo, J. Rivera-Utrilla, G. Prados-Joya, M.A. Ferro-Garcia, I. Bautista-Toledo, Water Research 42 (2008) 4163–4171.
[23] H. Shemer, Y.K. Kunukcu, K.G. Linden, Chemosphere 63 (2006) 269–276.
[24] Z. Zhang, N. Cissoko, J.J. Wo, X.H. Xu, Journal of Hazardous Materials 165 (2009) 78–86.
[25] Q.L. Wang, S.R. Kanel, H. Park, A. Ryu, H. Choi, Journal of Nanoparticle Research 11 (2009) 749–755.
[26] S. Bae, W. Lee, Applied Catalysis B-Environmental 96 (2010) 10–17.
[27] B.L. Cushing, V.L. Kolesnichenko, C.J. O'Connor, Chemical Reviews 104 (2004) 3893–3946.
[28] S. Choe, S.H. Lee, Y.Y. Chang, K.Y. Hwang, J. Khim, Chemosphere 42 (2001) 367–372.
[29] G.V. Lowry, K.M. Johnson, Environmental Science & Technology 38 (2004) 5208–5216.
[30] Q. Wang, S. Snyder, J. Kim, H. Choi, Environmental Science & Technology 43 (2009) 3292–3299.
[31] K. Sohn, S.W. Kang, S. Ahn, M. Woo, S.K. Yang, Environmental Science & Technology 40 (2006) 5514–5519.
[32] X.H. Xu, J.J. Wo, J.H. Zhang, Y.J. Wu, Y. Liu, Desalination 242 (2009) 346–354.
[33] H. Song, E.R. Carraway, Environmental Science & Technology 39 (2005) 6237–6245.
[34] J. Fan, Y.H. Guo, J.J. Wang, M.H. Fan, Journal of Hazardous Materials 166 (2009) 904–910.
[35] H. Tian, J.J. Li, Z. Mu, L.D. Li, Z.P. Hao, Separation and Purification Technology 66 (2009) 84–89.
[36] W.H. Zhang, X. Quan, Z.Y. Zhang, Journal of Environmental Sciences-China 19 (2007) 362–366.
[37] S.H. Joo, D. Zhao, Chemosphere 70 (2008) 418–425.
[38] W. Wang, Z.H. Jin, T.L. Li, H. Zhang, S. Gao, Chemosphere 65 (2006) 1396–1404.
[39] M.N. Amin, S. Kaneco, T. Kato, H. Katsumata, T. Suzuki, K. Ohta, Chemosphere 70 (2008) 511–515.
[40] H. Choi, S.R. Al-Abed, S. Agarwal, D.D. Dionysiou, Chemistry of Materials 20 (2008) 3649–3655.
[41] D. Colon, E.J. Weber, J.L. Anderson, P. Winget, L.A. Suarez, Environmental Science & Technology 40 (2006) 4449–4454.
[42] P. Larese-Casanova, M.M. Scherer, Environmental Science & Technology 42 (2008) 3975–3981.